MICRO-ANALYSIS ON THE INTERNAL STRUCTURE OF FIBRE-SOIL COMPOSITE

Humphrey Danso

Construction & Wood Technology Department, University of Education Winneba, P. O. Box 1277, Kumasi-Ghana

Corresponding author; e-mail: hdanso@uew.edu.gh / dansohumphrey@yahoo.co.uk

Abstract

Micro-structure of any composite material influences to a greater extent the performance properties of the material. The aim of this study is to investigate the internal structure of fibre-soil composite through micro-analysis for better understanding of the material's behavior. Soil and natural fibres were used to prepare fibre-soil composites and CT scan, SEM and optical microscopy analysis were conducted on the composites. The CT scan analysis found that pores and cracks exist in the fibre-soil composites, and the fibres are randomly distributed in the soil matrix with greater concentration at the middle portion. SEM analysis revealed that there is presence of gaps between the fibres and the soil matrix in the composite, with optical microscope analysis confirm the gaps to be 9-32, 31-51 and 53-119 µm, respectively for Bagasse, oil palm and coconut fibres. It was further revealed that the gaps are developed mainly due to the shrinkage of the fibres in the soil matrix. The study therefore concludes that fibre-soil composites develop internal micro-cracks, pores and micro gaps are formed between the fibres and the soil matrix. These identified features have the potential of influencing the performance properties of the fibre-soil composites. It is therefore recommended that further studies are conducted to assess the impact of these internal features on the properties of the fibre-soil composites.

Keywords:
Composite, fibres, micro-analysis, soil

1 INTRODUCTION

The existence of pores and micro-cracks have negative influence on the engineering properties of construction materials. In many modern engineering designs, materials with highly complex micro-structures are now in use [Zohdi & Wriggers 2001]. The use of surface geometry of any materials is difficult if not impossible to ascertain the internal structure, especially with composite materials. The microscopic-macroscopic relationship of the material is complex, and the micro-structure in the material has a great influence on its macroscopic characteristics [Guan, Wang, Liu, Wang & Luan 2017].

Building materials expose a variety of particles that cross a diversity of well-established micro-analysis specialty areas such as coatings, polymers, fibers, and glass [William & Schneck 2017]. Composite building materials usually have some bonding problems that affect the strength of the materials. Due to invisibility of the internal part of the materials, it is very difficult to identify the problem in order to take steps to improve upon the manufacturing process. Studies into fibre-soil composite have gain popularity in the recent time [Donkor & Obonyo 2016; Danso 2017, Danso et al. 2015a; Danso et al. 2015b]. However, the interaction between the fibres and soil matrix is complicated by the addition of water with each component differing in expansion resulting in relative dimensional changes upon drying and subsequent debonding [Danso et al., 2017].

According to Diambra et al. [2013] the technology of fibre reinforcement of soils has not been decisively adopted by formal building sector because of the lack of the understanding of the interaction mechanism between the soil and the fibre. There is therefore the need to study the interaction between fibres and soil matrix in order to gain knowledge about the internal structure of the composite. The aim of this paper is to investigate the internal structure of fibre-soil composite through micro-analysis for better understanding of the material's behavior.

2 MATERIALS AND METHODS

2.1 Materials

The principal materials used for the study are soil, natural fibres and water. The soil sample was obtained from Horsea Island, Portsmouth England, United Kingdom. The site was cleared of all bushes, shrubs, hedges and trees. Top soil was removed to depth of about 300mm because they contain organic matter and have low bearing capacity which makes it unsuitable for construction purposes. The soil sample was dug and sieved through a 10 mm sieve for bigger particles and unwanted materials be removed and allowed to dry. The optimum moisture content (OMC) and maximum dry

density (MDD) of the soil sample are 11.8% and 1.83Mg/m^3, respectively. The particle size distribution (grading) of the soil is presented in Fig. 1. The liquid limit, plastic limit and plasticity index of the soil are 31.7(%), 18.9(%) and 13.7(%) respectively.

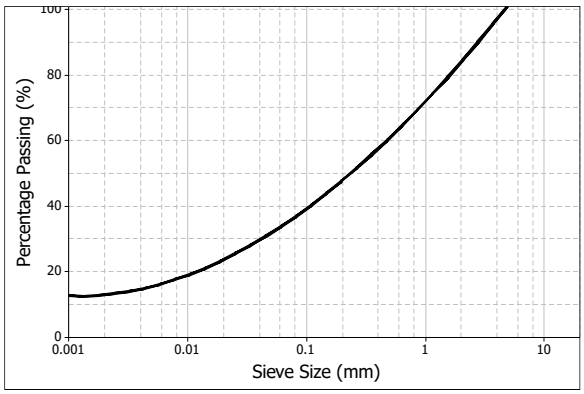

Fig. 1: Particle size distribution of the soil sample

Fibres were obtained from three different agricultural wastes (sugarcane residue 'bagasse', coconut husk and oil palm fruit residue) in Ghana. Tab. 1 shows the lengths and diameters of one hundred each of coconut, oil palm and bagasse fibres. Fig. 2 shows the images of the fibres. Tap water from the civil engineering laboratory of University of Portsmouth, UK was used for making the blocks.

Tab 1: Lengths and diameters of fibres (n=100)

	Length (mm)		Diameter (mm)	
Fibre	Mean	Std. Dev.	Mean	Std. Dev.
Bagasse	110.30	28.93	0.78	0.19
Oil palm	38.01	6.49	0.38	0.08
Coconut	102.98	17.94	0.40	0.17

Bagasse fibre Coconut fibre Oil palm fibre

Fig 2: Photographs of the fibres

2.2 Methods

2.2.1 Specimens Preparation

Soil, 1% fibre by weight and 11.8% water (as obtained by OMC) were used for making the specimens. The soil was first measured and spread on a platform, then the fibre was measured and spread on soil and turned over and over until a uniform mixture was obtained. The required water was sprinkled on the soil-fibre mixture and turned over and again to obtain a homogenous mixture. Cylindrical specimens of 80 mm length × 40 mm diameter (Fig. 3) were prepared by placing 200 g of the mixture into a cylindrical mould with 40 mm internal diameter and 125 mm length and quasi-statically compressing at 10 MPa pressure to a length of 80 mm, using a close fitting piston with a Tinius Olsen H50KS. These specimens were used to find out the distribution of the fibres in the soil matrix. 50 mm cube specimens (Fig. 3) were prepared with a steel mould with internal dimension 50×50×50 mm and compressed at 10 MPa pressure with a Tinius Olsen H50KS. One mould was placed on the other which allowed the mixture to be placed in and compressed to 50 mm with a wooden plate on top. The cubes were used to determine the gaps between the fibres and the soil matrix. All the specimens were dried in fan assisted Genlab electronic oven at a temperature of 40 °C for five days when the mass stabilised.

Fig 3: Cube and cylindrical specimen

2.2.2 Test Procedure

This section describes the test procedure performed on the specimens. The tests conducted include CT scan, SEM and optical microscopy. A computerised tomography (CT) scan analysis was conducted to find out the distribution of the fibres in the soil matrix. Metric XT H 225 Microfocus CT Scanner was used to scan the cylinder and cube specimens. The CT scan produced images (slides) which was modelled with VGStudio MAX version 2.0 to produce the 3D result of the specimens showing the orientation of the fibres. Scanning electron microscopy (SEM) and optical microscope analysis were conducted to determine whether gaps exist at the peripheral of the fibres in the specimens. Selected cubes were broken to expose the internal parts for the analysis with JSM-6100 scanning microscope (Fig. 4a) and computerised optical microscope (OLYMPUS BX40) with Leica Application Suite version 3.4.0 (Fig. 4b). To determine whether the gaps were caused by shrinking of the fibres or the soil matrix, twenty-five fibres from each fibre type were randomly selected and measured in dried state and wet state after immersing in water for 48 hours.

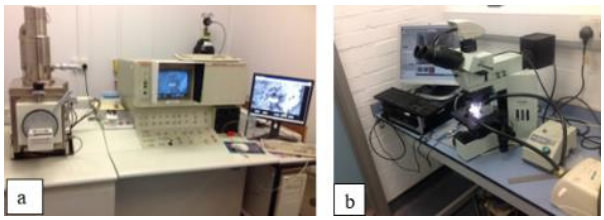

Fig 4: Analysing specimens for gaps with (a) JSM-6100 scanning microscope, (b) OLYMPUS BX40 computerised optical microscope

3 RESULTS AND DISCUSSION

3.1 CT Scan Analysis

The results obtained for cube specimens (Fig. 5) can clearly show three main important features of the fibre-soil composite which the naked eyes could not see from the physical examination of the composite. This was due the fact that the images provided from the Fig. 5

were captured from internal part the specimens. The three features are:

1. The soil matrix which consist of grey colour (clay, silt and sand constituents) and white colour (gravel constituent)

2. Pores in the composite shown by black spots

3. Cracks in the composite shown by continuous linear dark patterns

Conspicuously missing in the composite is the fibre. The CT scanner could not capture the fibres in the block due to the low specific weight of the fibres. Due to this, lower density lens setting was adopted for the cylindrical specimen scanning.

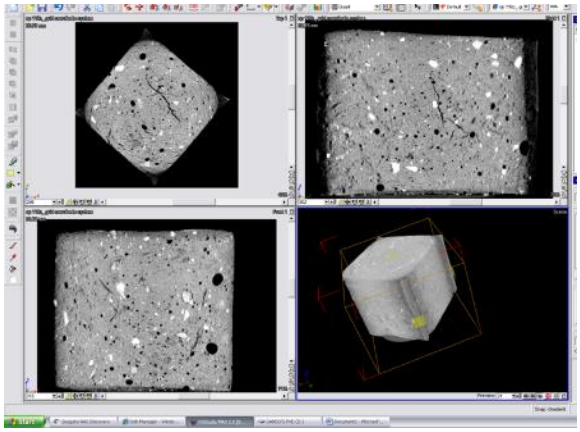

Fig. 5: Images from CT scan (cube specimens)

For better understanding of the cracks shown by the images (since they could not be seen on the composite with the naked eyes) computer modeling on the CT scan images was conducted. Computational modeling with VGStudio MAX version 2.0 was performed on the images produced by the CT scan to obtained 3D images. 794 slices were obtained from the one composite TC scan, which was used to model the composite (Fig. 6a). The image was moved to slice 1 to view the features in front of the composite as can be seen in Figure 6b. The image was the moved to slice 397 (Figure 6c) which is the middle of the composite to view the details. At this stage the image was view in different 3D orientations (Fig. 6d), thus XYZ, ZXY and YZX.

From the results, it can be observed that the external surface (Fig. 6b) of the composite had features such as soil matrix and pores in grey/white and black coloures, respectively. As the slice was moved to the middle of the block (Fig. 6c), a critical observation shows diagonal cracks. This implies that though the external surfaces of the composite do not show cracks, there are cracks developed inside. These cracks are usually developed due to the presence of clay content in the soil [Arumala & Gondal 2007] and rapid and non-uniform drying [Ghavami et al. 1999]. It can therefore be assumed that the greater the clay content, the more likely the composite may develop internal crack even if not shown on the external surface of the composite.

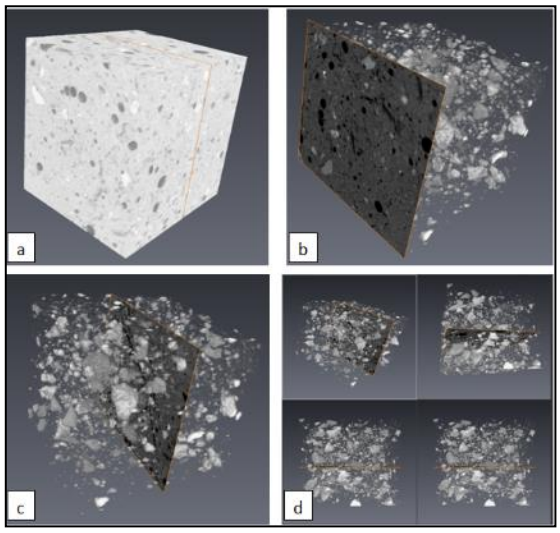

Fig. 6: D Images from Modelled scan slices (cube specimen)

As can be seen from Fig. 7, the external part of the specimen had few fibres. This means that the soil matrix provides a cover for the fibres as in the case of reinforced concrete where cover is deliberately created to protect the reinforcement bars from the effect of the weather. It can be observed however that, the greater fibre concentration is within the internal part of the specimen, and the fibres are fairly distributed.

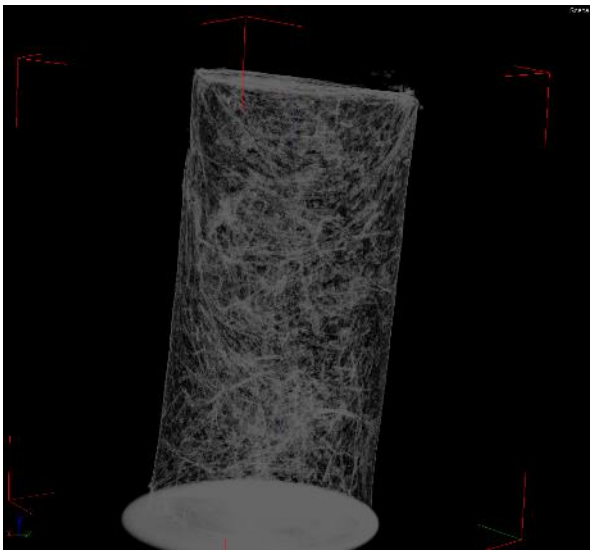

Fig. 7: D Images from Modelled scan slices (cylindrical specimen)

3.2 Scanning Electron Microscopy (SEM) Analysis

The results obtained from the SEM analysis are presented in Fig. 8, Fig. 9 and Fig. 10 respectively for sugarcane Bagasse, coconut and oil palm fibres soil composite. Fig. 8 illustrates the spatial relationship between sugarcane Bagasse fibres and the soil matrix. It can be observed in B1 that after the composite is dried, very little gaps are created between the fibre and the soil matrix. However, the image in B2 (showing the section of broken sugarcane Bagasse fibre in the soil matrix) shows a number of pores in the fibre. This suggests that for Bagasse fibres, there are little gaps created between the fibres and soil after drying, but there are number of pores developed within the fibre. Furthermore, it can be observed from Fig. 8 that there is an increase in the roughness of fibre, which can

contribute with the increase of the interfacial bonding between fibre and soil matrix [Rodrigues et al. 2011].

In Fig. 9, the relationship between coconut fibres and the soil matrix are shown. It can clearly be seen from C1 and C2 images that there are spaces between the peripheral of the fibres and the soil matrix. The spaces look bigger than that of the Bagasse fibre and soil, implying that the swelling and shrinking effect on the coconut fibre is more pronounced. However, it was observed that few and very small pores were within the coconut fibres. This implies that though there is dimensional effect of fibres due to swelling and shrinkage, the fibres are denser and stronger which could have impact on the strength and durability properties of the composite. The image in C1 further shows the distribution of the coconut fibres in the soil matrix, which indicate fibres in both longitudinal and cross sections.

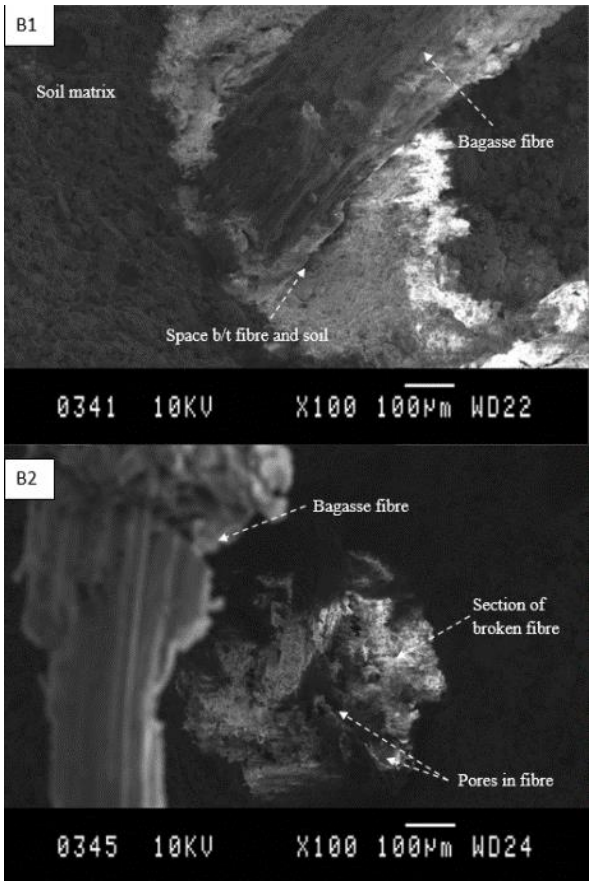

Fig. 8: SEM micrographs of Bagasse fibre-soil composite

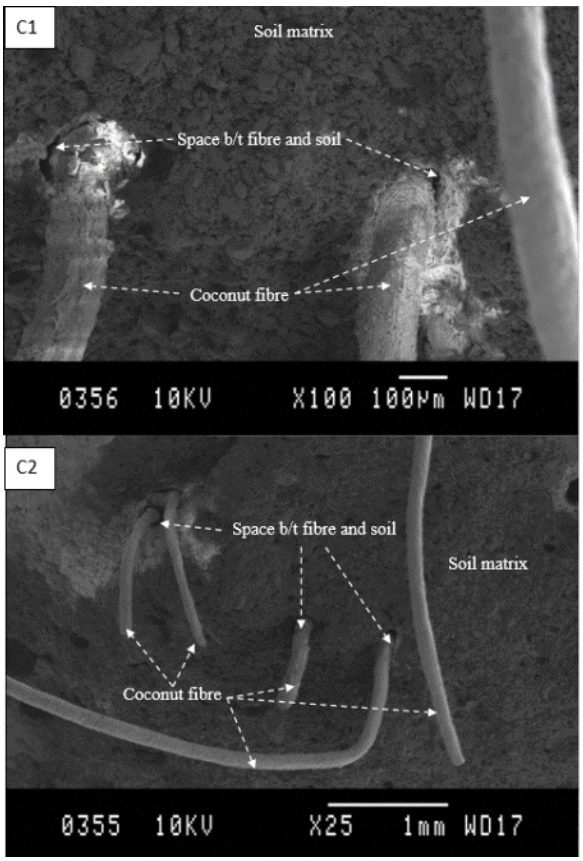

Fig. 9: SEM micrographs of coconut fibre-soil composite

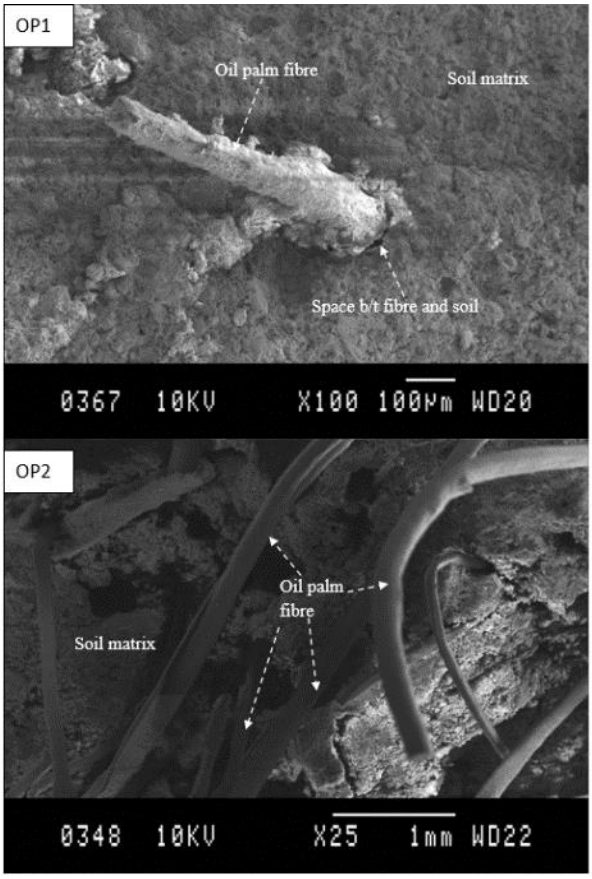

Fig. 10: SEM micrographs of oil palm fibre-soil composite

This suggests that the fibres are distributed in different orientations which could ensure good interlocking of the soil matrix and can have impact on the wearing and

erosion of the composite. For oil palm fibres, similar result was obtained as shown in Fig. 10. As expected, there were gaps formed between the peripheral of the fibre and the soil matrix as can be observed from OP1. The gaps are similar to those in the coconut fibre soil blocks. The image in OP2 shows the distribution of the oil palm fibres in the soil.

3.3 Optical Microscope Analysis

The SEM analysis could only show the micro-structure of the composite, without providing numerical data about gaps between the fibres and the soil matrix. Optical microscope was therefore used to measure the gaps between the fibres and the soil matrix. The results obtained are presented in Fig. 11, Fig. 12 and Fig. 13, respectively for Bagasse, oil palm and coconut fibres soil composite. Fig. 11 shows the internal relationship between sugarcane Bagasse fibres and the soil matrix. Images from B1 row provide the fibre in the soil at 25X magnification which show close contact between the fibre and the soil matrix as was also identified in the SEM images. Images from B2 row provide the measured gaps between the fibres and the soil matrix. It can be seen that the spaces are between about 9 µm and 32 µm. This range of gaps is the lowest as compared to the oil palm and coconut fibres-soil composite. This confirms the result from the SEM that there is increase of the interfacial bonding between sugarcane Bagasse fibre and soil matrix [Rodrigues et al. 2011], which could be attributed to the increase surface roughness of the sugarcane Bagasse fibre.

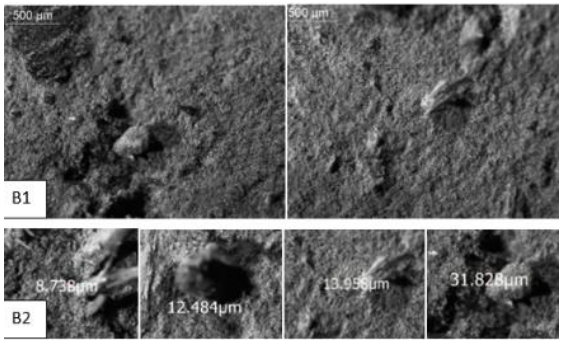

Fig. 11: Optical microscope images of Bagasse fibre-soil composites

The relationship between oil palm fibres and the soil matrix are shown in Fig. 12. The images in OP1 row show the fibre in the soil which illustrates some vivid gaps between the fibre and the soil matrix as also identified in the SEM analysis. Images in OP2 row provide the measured gaps between the fibres and the soil matrix. The gaps measured were between approximately 31 µm and 51 µm. These spaces are found to be bigger than those in the Bagasse fibre-soil composite; however, they are smaller as compare to those in coconut fibre-soil composite.

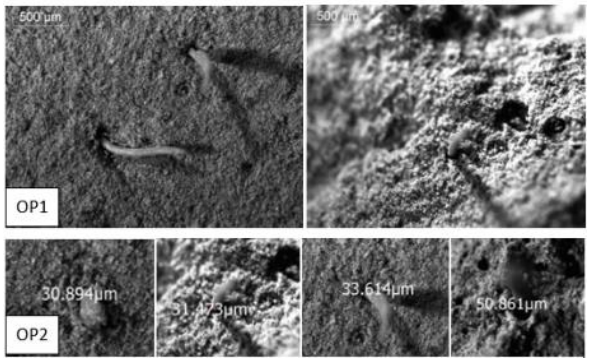

Fig. 12: Optical microscope images of oil palm fibre-soil composites

In Fig. 13, the relationship between coconut fibres and the soil matrix are shown. The images in C1 row show the fibres in the soil which illustrate clear gaps between the peripheral of the fibres and the soil matrix as also identified in the SEM analysis. Images in C2 row present the measured spaces between the fibres and the soil matrix. The spaces measured were between approximately 53 µm and 119 µm. These gaps are bigger than those in both the sugarcane Bagasse and coconut fibre-soil composites.

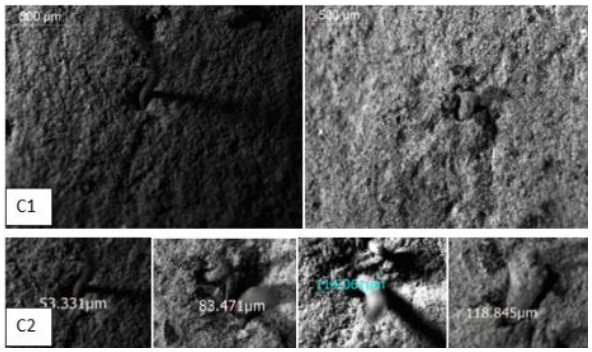

Fig. 13: Optical microscope images of coconut fibre-soil composites

A quantitative approach was adopted to find out the fibre gap-diameter percentage. The summary of the results is presented in Tab. 2. The results indicate that Bagasse fibre obtained the lowest fibre gap-diameter percentage, followed by oil palm and the highest been coconut fibre. This confirms the closeness of Bagasse fibre interfacial bonding with soil matrix as was observed in the scan images, as compared to oil palm and coconut fibres.

Tab. 2: Fibre gap-diameter percentage (n=25)

Fibre	Mean Gap (mm)	Mean Diameter (mm)	Gap/Diameter (%)
Bagasse	0.018	0.80	2.30
Oil palm	0.038	0.38	10.00
Coconut	0.077	0.40	19.30

3.4 Mechanism of Fibres in Soil Matrix

The mechanism of the fibres and the soil matrix is important to describe the behavior of the fibres in soil matrix. The fibre and soil matrix relationship has been found to be governed by three main factors [Ghavami et al. 1999; Hejaz et al. 2012]; the shear resistance of the soil due to the surface form and roughness of the fibre, the compressive friction forces on the surface of the

fibre due to shrinkage of the soil, and the cohesive properties of the soil.

Each of these factors is generally affected by the dimensional changes of the fiber which can occur due to changes in moisture and temperature [Ghavami et al. 1999]. The changes in fibre dimension occur during the drying of the fibre enhanced soil blocks which determines a possible mechanism resulting in a poor interfacial bond [Hejaz et al. 2012]. At the mixing stage of the materials, the fibres absorb water which cause the fibres to expand or swelling and at the drying stage, the fibres shrink creating spaces (pores/voids) between the fibres and the soil matrix as illustrated in Figs. 14 and 15. This behavior of the fibres in the soil can weaken the bond between the fibres and the soil matrix [Ghavami et al. 1999; Hejaz et al. 2012; Segetin et al. 2007].

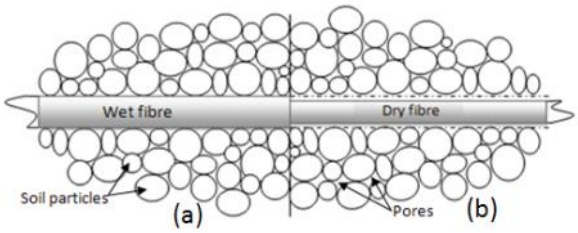

Fig. 14: Longitudinal sketch of fibre in soil matrix: (a) in wet condition and (b) in dry condition

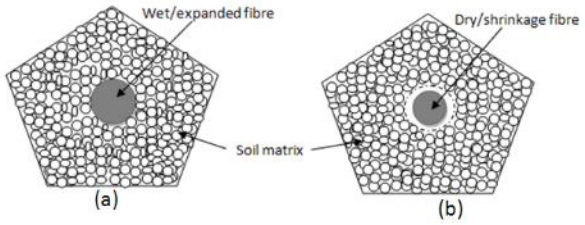

Fig. 15: Cross-sectional sketch of fibre in soil matrix: (a) in wet condition and (b) in dry condition

Another important property of fibre that contributes to the bond between the fibres and the soil matrix is the texture of the fibre. When there is increase in the roughness of fibre, it can contribute to the increase of the interfacial bonding between fibre and soil matrix [Rodrigues et al., 2011]. The bond between the fibre and the matrix when increased will minimize the voids between the fibre and the matrix. This might have contributed to the Bagasse fibre obtaining small voids between the fibres and the soil matrix as compare to coconut and oil palm fibres. When the voids between the composites are large, it contributes to pull out effect of the fibres from the matrix which results in adhesion failure [Luz et al. 2007] and this defect is prominent at high fibre content [Cao et al. 2006].

To better and fully understand the mechanism of the fibres in the soil matrix, the study further examined the fibres diameter when dried and saturated. This approach was informed by the method used in this study, where the fibres were kept in water until saturation before mixed with soil. Summary of the results is shown in Tab. 3.

Tab. 3: Diameters of dry and wet fibres (n=25)

Fibre	Mean Dry Diameter (mm)	Mean Wet Diameter (mm)	Diff. in Diameter (mm)
Bagasse	0.707	0.733	0.026
Oil palm	0.359	0.407	0.048
Coconut	0.457	0.542	0.085

The result shows that there were 0.026, 0.048 and 0.085 mm difference in diameter respectively for bagasse, oil palm and coconut fibres between the average dry and saturated diameters. This follows the trend in the gaps identified in the blocks between the fibres and the soil matrix. However, the difference in diameter obtained between the dry and saturated fibres were bigger than the gaps identified in the composites. This could be explained that, when the fibres are kept in water, they absorb moisture and therefore expand and when mixed with soil and compacted the fibres undergo a bit of shrinkage due to the pressure, and further shrink when the composites are dried. This means that there are two stages that the fibres shrink; (1) shrinkage due to the compaction force when making the blocks, and (2) shrinkage due to drying of the blocks. Meaning the gaps found in the optical microscope analysis represent the gaps created by the drying of the composites (second shrinkage). It must be noted that these two shrinkage stages are all caused by loss of absorbed water in the fibres, which is the difference in dry and saturated fibre diameter. Implying that the fibres expand when kept in water and shrink to its natural diameter through compaction and drying of the composite.

4 CONCLUSION

This paper aimed at investigating the internal structure of fibre-soil composite through micro-analysis for better understanding of the material's behavior. In order to achieve this, CT scan, SEM and optical microscopy analysis were conducted on the fibre-soil composite. The CT scan analysis found that pores and cracks exist in the fibre-soil composite which the naked eye cannot see, and the fibres are randomly distributed in the soil matrix with greater concentration at the middle portion. SEM analysis revealed that there is presence of gaps between the fibres and the soil matrix in the composite, with optical microscope analysis confirm the gaps to be 9-32, 31-51 and 53-119 µm, respectively for Bagasse, oil palm and coconut fibres. It was further revealed the gaps are developed mainly due to the shrinkage of the fibres in the soil matrix. The study therefore concludes that fibre-soil composites develop internal micro pores, cracks and micro gaps are formed between the fibres and the soil matrix. These identified features have the potential of influencing the performance properties of the fibre-soil composites. It is therefore recommended that further studies are conducted to assess the impact of these internal features on the properties of the fibre-soil composites.

5 REFERENCES

Al-Sakkaf, Y. K. A. (2009). Durability Properties of Stabilized Earth Blocks. PhD. Thesis Universiti Sains Malaysia.

Arumala, J. O. & Gondal, T. (2007). Compressed Earth Building Block for Affordable Housing, London, United Kingdom, RICS Publishers.

Beglarigale, A. & Yazıcı, H. (2015). Pull-out behavior of steel fiber embedded in flowable RPC and ordinary mortar. *Construction and Building Materials,* 75**,** 255–265

Cao, Y., Shibata, S. & Fukumoto, I. (2006). Mechanical properties of biodegradable composites reinforced with bagasse fibre before and after alkali treatments. Composites Part A: Applied Science and Manufacturing, 37, 423–429

Danso, H., Martinson, B., Ali, M. & Williams, J. B. (2017). Mechanisms by which the inclusion of natural fibres enhance the properties of soil blocks for construction. Journal of Composite Materials, 51(27), 3835–3845.

Danso, H. (2015). Use of agricultural waste fibres as enhancement of soil blocks for low-cost housing in Ghana. University of Portsmouth, http://eprints.port.ac.uk/id/eprint/20762

Danso, H., Martinson, D.B., Ali, M. & Williams, J.B. (2015a). Physical, mechanical and durability properties of soil building blocks reinforced with natural fibres. Construction and Building Materials, 101, 797-809, 2015.

Danso, H., Martinson, B., Ali, M. & Williams, J. B. (2015b). Effect of sugarcane bagasse fibre on the strength properties of soil blocks. In: 1st International conference on bio-based building materials, Clermont-Ferrand, France, 22–24 June 2015, pp.251–256.

Donkor, P. & Obonyo. E. (2016). Compressed soil blocks: Influence of fibers on flexural properties and failure mechanism. Construction and Building Materials, 121: 25–33.

Diambra, A., Ibraim, E., Russell, A. R. & Muir Wood, D. (2013). Fibre reinforced sands: from experiments to modelling and beyond. International Journal for Numerical and Analytical Methods in Geomechanics, 37, 2427–2455.

Ghavami, K., Filho, R. D. T. & Barbosac, N. P. (1999). Behaviour of composite soil reinforced with natural fibres. Cement and Concrete Composites, 21, 39-48.

Guan, Y., Wang, E., Liu, X., Wang, S. & Luan, H. (2017). The Quantified Characterization Method of the Micro-Macro Contacts of Three-Dimensional Granular Materials on the Basis of Graph Theory. Materials, 10,898, 1-18.

Hejazi, S. M., Sheikhzadeh, M., Abtahi, S. M. & Zadhoush, A. (2012). A simple review of soil reinforcement by using natural and synthetic fibres. Construction and Building Materials 30, 100-116.

Luz, S. M., Goncalves, A. R. & Del'arco Jr., A. P. (2007). Mechanical behavior and microstructural analysis of sugarcane bagasse fibers reinforced polypropylene composites. Composites Part A: Applied Science and Manufacturing, 38, 1455–1461

Medjo Eko, R., Offa, E. D., Ngatcha, T. Y. & Minsili, L. S. (2012). Potential of salvaged steel fibers for reinforcement of unfired earth blocks. Construction and Building Materials, 35, 340–346

Medjo Eko, R. & Riskowski, G. (1994). Effects of fibers and cement on the mechanical behavior of soil–cement reinforced with sugar cane bagasse. Housing Sci 18:79–89.

Millogo, Y., Morel, J.-C., Aubert, J.-E. & Ghavami, K. (2014). Experimental analysis of pressed adobe blocks reinforced with hibiscus cannabinus fibers. Construction and Building Materials, 52, 71–78

Rodriguez, M. A. & Saroza, B. (2011). Determination of the optimum composition of adobe brick for a school in Cuba. Materiales Construccion, 56, 53-62.

Rivera-Gómez, C., Galán-Marín, C. & Bradley, F. (2014). Analysis of the Influence of the Fiber Type in Polymer Matrix/Fiber Bond Using Natural Organic Polymer Stabilizer. *Polymers, 6*, 977-994; doi:10.3390/polym6040977

Segetin, M., Jayaraman, K. & Xu, X. (2007). Harakeke reinforcement of soil–cement building materials: manufacturability and properties. *Build Environ, 42*, 3066–79.

Tuyan, M. & Yazıcı, H. (2012). Pull-out behavior of single steel fiber from SIFCON matrix. Construction and Building Materials 35, 571–577, doi:10.1016/j.conbuildmat.2012.04.110.

William, M. & Schneck. M.S. (2017). Forensic Microanalysis of Building Materials. Washington State Patrol Crime Laboratory, https://projects.nfstc.org/trace/docs/final/Schneck.pdf

Zohdi, T.I. & Wriggers, P. (2001). Computational Micro-macro Material Testing. Archives of Computational Methods in Engineering, 8(2), 131-228.